Inhibition of the Effect of Some Carcinogens by Their Partially Hydrogenated Derivatives

It has been observed in various fields of biochemistry that a biologically active compound—for example, a vitamin—may be prevented from displaying its effect in the presence of a closely related derivative (antivitamin). The latter probably plays the part of a competitor for intracellular receptors.

The basic idea of our work (*1*) was to investigate whether or not the simultaneous injection of a strong carcinogen and a close derivative that differs from the carinogen by the level of oxidation only would prevent the appearance of malignant tumors. Evidently these experiments had to be conducted under conditions that secured a high tumor incidence in the absence of the added compound.

For this purpose, some reduction products of 20-methylcholanthrene and of 1,2,5,6-dibenzanthracene were prepared by partial and by total catalytic hydrogenation (*2*) and subsequent chromatographic resolution. Thus, methylcholanthrene yielded the 6,7-dihydro and the 1,2,3,4,11,14-hexahydro derivatives that were described earlier by Fieser and Hershberg (*3*), as well as the fully hydrogenated perhydromethylcholanthrene. Starting from dibenzanthracene, a dihydro, a decahydro, and the perhydro derivatives were obtained; however, the structure of the two partially hydrogenated compounds cannot be established with certainty at the present time. The decahydro compound melts sharply at 176°C, while the dihydro derivative is possibly a mixture of isomers.

In each instance, 30 male C57 mice, 3 to 4 months old were treated (*4*). They were kept on a standard commercial chow diet supplemented with rolled barley and were given water *ad libitum.*

The subcutaneously injected ethyl laurate solution (single injection) contained 30 μg (1 part) of carcinogen (TD$_{75}$) and 15 parts of hydrogenated carcinogen. The experiments were allowed to continue for 12 months.

The results are summarized in Table 1; all tumors listed there were subcutaneous spindle cell sarcomas. Table 1 demonstrates that while the addition of the fully hydrogenated substances had no influence on the carcinogenic potency, some partially reduced derivatives were highly effective in decreasing the tumor incidence. Thus, in the methylcholanthrene series, the tumor yield was decreased from 28 percent to 8 percent. In the case of dibenzanthracene, the results were more striking since its partially hydrogenated derivatives completely inhibited the tumorigenic power of the parent compound.

The incidence data reported are in good accordance with some other features. Indeed, an association may be observed between the tumor yield, tumor induction period, intervals of subsequent tumor formation, and the chemical nature of the hydrogenates. Table 1 shows that the presence of hexahydromethylcholanthrene not only decreased the number of observed tumors from 8 to 2 but also lengthened the induction period from 21 to 31.5 weeks. Furthermore, the interval between the first and the second tumor was extended from 0 to 18 weeks.

Although the available data are not extensive enough for a broad generalization, it is clear that in the series of polycyclic carcinogens a strong inhibiting effect of partially reduced derivatives does exist and that it reaches its optimum at a certain hydrogenation level. The weak effect of dihydromethylcholanthrene may be understood on the basis of its slight structural difference from methylcholanthrene and hence by its possible *in vivo* conversion into the carcinogen. In contrast, the inertness of the two fully hydrogenated substances studied could well be explained by the circumstance that since they are void of aromatic character and are no longer close derivatives of the parent compound, they cannot act as anticarcinogens in the tissue.

Our results are in line with some related data, especially with the concept of competition between carcinogens and anticarcinogens for available intracellular receptors (*5*).

Table 1. Inhibition and retardation of the carcinogenic effect of 20-methylcholanthrene and of 1,2,5,6-dibenzanthracene by some hydrogenated derivatives.

Compound	No. of animals	Survivors at time of first tumor	No. of tumors	Sequence of tumor appearance (wk)
20-Methylcholanthrene (MC)	30	29	8	21, 21, 21, 22, 22.5, 27.5, 28.5, 34.5
6,7-Dihydromethylcholanthrene + MC	30	29	6	18, 18, 18.5, 19, 26, 50.5
1,2,3,4,11,14-Hexahydromethylcholanthrene + MC	30	30	2	31.5, 49.5
Perhydromethylcholanthrene + MC	30	30	7	14.5, 18, 27.5, 27.5, 28, 31.5, 33
1,2,5,6-Dibenzanthracene (DB)	30	29	7	19, 25.5, 27, 29, 32, 39, 43
Dihydrobenzanthracene + DB	30	30	0	none
Decahydrobenzanthracene + DB	30	29	0	none
Perhydrobenzanthracene + DB	30	30	5	27, 34, 40, 42, 44

PAUL KOTIN
HANS L. FALK

Departments of Pathology and Biochemistry, University of Southern California School of Medicine, and the Laboratories, Los Angeles County General Hospital

W. LIJINSKY
L. ZECHMEISTER

Gates and Crellin Laboratories of Chemistry, California Institute of Technology, Pasadena

References and Notes

1. This research was supported in part by an institutional grant from the American Cancer Society to the University of Southern California School of Medicine, and in part by a grant of the Damon Runyon Memorial Fund to California Institute of Technology.
2. For some experimental conditions, see W. Lijinsky and L. Zechmeister, *J. Am. Chem. Soc.* 75, 5495 (1953).
3. L. F. Fieser and E. B. Hershberg, *ibid.* 60, 940 (1938).
4. The mice were obtained from the Cancer Research Genetics Laboratory, Berkeley, Calif.
5. H. G. Crabtree, *J. Pathol. Bacteriol.* 51, 303 (1940); A. Lacassagne, Buü-Hoi and G. Rudali, *Brit. J. Exptl. Pathol.* 26, 5 (1945); W. T. Hill *et al., Cancer Research* 11, 892 (1951); P. E. Steiner and H. L. Falk, *ibid.* 11, 56 (1951).

5 August 1955

Two Methods of Obtaining Least Squares Lines

S. I. Askovitz reported a method for determining the mean y value ($\bar{y}$) from graphic data (*1*). Two methods of obtaining the best fitting straight line through a set of points are presented here. The first method uses the Askovitz technique to find $\bar{y}$, while the slope is calculated from the values of y on a transposed x-axis. The second method is, to my knowledge, original and is completely graphic. In it, two points of the best fitting line are found directly on the graph. In each case, if the original data are in the form of a continuous curve, discrete values of x must be chosen, and the same limitation holds as in Askovitz' method, namely, that the individual points must be at equal intervals of x.

First method. A modification of the method of Arkin and Colton (*2*) is used —that is, when there are an odd number

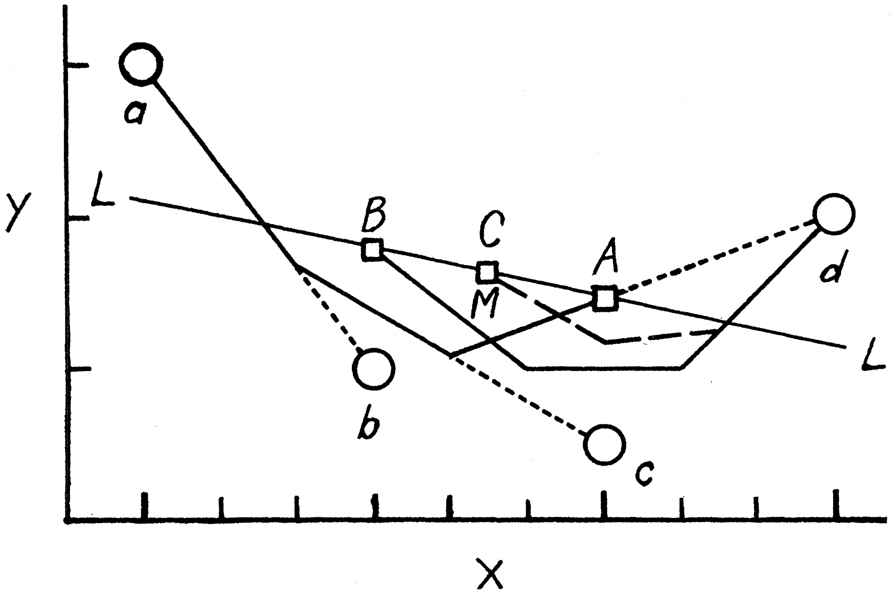

Fig. 1. The least squares line for the points *a, b, c,* and *d* is *LL*. The mean *y* value is at *C*. *A* is the balance point for the centroid weighted as $a=1$, $b=2$, $c=3$, and $d=4$. *B* is the balance point for the centroid weighted as $a=4$, $b=3$, $c=2$, and $d=1$. *M* is the midpoint of the line segment *AB*. The dotted and solid lines show the graphical way of determining *A* and *B*. The dashes show the graphical way of determing the check point *C*.

of points plotted, the origin of the abscissa is shifted to the middle point of the set. To the left of the origin, the points are numbered -1, -2, -3, and so forth, and to the right they are numbered $+1$, $+2$, $+3$, and so forth. If there are an even number of points, a point on the abscissa midway between the middle points is made the origin. To the left of this origin, the values are taken as -1, -3, -5, and so forth; to the right they are taken as positive odd integers.

The *y* value of each point is multiplied by its new corresponding *x* value. The sum of these products is divided by Σx^2. A table for the values of Σx^2 can be computed from Eq. 1 and Eq. 2. When *n* is odd

$$\Sigma x^2 = \frac{n(n^2-1)}{12} \quad (1)$$

and when *n* is even,

$$\Sigma x^2 = \frac{n(n^2-1)}{6} \quad (2)$$

where *n* is the number of points in the set and *x* is the transposed abscissa value of the point. The Σx^2 terms of Eq. 2 are already corrected for having been placed on a transposed axis and computed in units of $x/2$.

Second method. Referring to the uniform distance between points as a "unit," proceed as follows (Fig. 1). Align a straightedge with the first (*a*) and second (*b*) points of the data. Place the point of a pencil along the straightedge, two-thirds of a unit from *a* toward *b*. Then align the edge with the pencil point and the third point (*c*). Lift the pencil and place it at a new pivot two-thirds of a unit from the first pivot. Realign the edge with the pencil and the next point of the data and continue in a similar manner until all the points have been used. The last pivot mark will be two-thirds of the total distance on the abscissa beween the first and last points of data. A corresponding terminal pivot point is obtained by beginning at the other end of the data and working back in steps of two-thirds of a unit. A line drawn through these two terminal points is the least squares line for the data considered. A simple check for errors may be made by graphically determining the $\bar{y}$ value by Askovitz' method (*1*)—that is, starting from either end of the data and moving by steps of one-half unit, a midpoint is obtained that is also on the best fitting line.

In the cases where it is known that the least squares lines should pass through point *a* (as in standard curves that are properly corrected for blank values), the construction simplifies to the following: start at point *b*, and progress by steps of two-thirds of a unit through all the remaining points. The termination is a point Ω that may be connected with *a* to give the best fitting line through this origin. Note that Ω and its reversed counterpart may also be used equally well in constructing the line *AB*, since the points lie on the original least squares line one-third of a unit beyond *A* and *B*, respectively.

In actual practice, when one uses decimal graph papers (preferably with accented lines every five divisions), it is convenient to choose a unit distance equal to either 15 or 30 of the smallest divisions. In this manner, moving two-thirds of a unit between pivot points always brings one to an accented line that facilitates the rapid execution of the maneuvers. On the other hand, if it is more important to make the unit a multiple of 10 for subsequent interpolations of *x* values, the unit may be taken as 20 of the smallest divisions. Here, 13 divisions between pivot steps will yield a line that is a very close approximation to the least squares line. It is suggested that if this graphic method of least squares lines becomes popular, the manufacturers of graph papers might consider producing a new design in which there would be two lines of a second color placed one-third and two-thirds of the distance between each unit of ten divisions. Such a paper would have the advantages of decimal convenience as well as ease of finding the pivot points.

Proof of second method. Let there be a set of *n* points designated 1,2,3 . . . n_i . . . *n*, with *x* (on the transposed abscissa as in the first method) and *y* values for the individual points. Let α be the centroid composed of the plotted points of data but with each point weighted per its n_i value, starting from left to right. Let β be the centroid weighted per

$$n+1-n_i$$

(that is, from right to left), while γ represents the centroid in which all points have equal weight. *A, B,* and *C* will be the balance points of the centroids α, β, and γ, respectively, and *M* will be the midpoint of the line segment *AB*. It is shown that point *C* coincides with *M* as follows:

$$x_C = 0$$

and *C* lies on the least squares line, while

$$y_A = \bar{y}_\alpha$$
$$y_B = \bar{y}_\beta$$

and

$$y_C = \bar{y}_\gamma$$

As in Askovitz' method, but with weighted values, the balance point *A* is reached at two-thirds of the distance ($n-1$ units) from point 1 toward *n*, and point *B* is reached two-thirds of the way from *n* toward 1. It follows, then, that *A* and *B* are one-third of $(n-1)$ units apart and that the midpoint of the line *AB* is on the line $x=0$. Since α and β are arithmetic step wedges in opposite directions and with equally weighted extremes, superimposing these congruent centroids will result in a composite centroid with a balance point *M* midway between *A* and *B*. Each point in the new centroid, however, has a weight equal to

$$n_i + (n+1-n_i) = n+1$$

Therefore, M is the balance point of an equi-weighted centroid and coincides with C. The slope of the line AB is

$$3\left(\frac{\bar{y}_\beta - \bar{y}_a}{n-1}\right)$$

and that of the best fitting line is $\Sigma xy/\Sigma x^2$.
Substituting the proper values gives

$$\frac{3\left(\frac{\Sigma n_i y}{\Sigma n_i} - \frac{\Sigma[y(n+1-n_i)]}{\Sigma n_i}\right)}{n-1} = \frac{\Sigma xy}{\Sigma x^2} \quad (3)$$

When n is odd, Eq. 3 leads through

$$\frac{\Sigma n_i}{2}\left(\Sigma\left[y\left(x+\frac{n+1}{2}\right)\right] - \Sigma\left[y\left(\frac{n+1}{2}-x\right)\right]\right) = \Sigma xy \Sigma\left(x+\frac{n+1}{2}\right) \quad (4)$$

to

$$\Sigma n_i \Sigma xy = \Sigma n_i \Sigma xy$$

When n is even, Eq. 3 leads through

$$2\Sigma[y(x+n+1)/2] - (n+1)\Sigma y = \Sigma xy \quad (5)$$

to

$$\Sigma xy = \Sigma xy$$

IRVING H. SHER
Research Laboratories, National Drug Company, Philadelphia, Pennsylvania

References and Notes

1. S. I. Askovitz, *Science* 121, 212 (1955).
2. H. Arkin and R. R. Colton, *Statistical Methods* (Barnes and Noble, New York, ed. 4, rev., 1950), pp. 56–60.

5 August 1955

Gases in Icebergs

Pure ice in thick layers is bluish in color, whereas an iceberg is typically white. The whiteness is caused by tiny, closely spaced gas cavities that are dispersed all through the ice. The cavities are often elongated and oriented lengthwise; this gives a grain to the ice. The gas is usually under pressure and is liberated with a fizzing sound when a piece of berg ice melts in a pail of water. With a lens one may watch the bubbles suddenly enlarge and pop out of their cavities when the walls melt open. The pressure is also manifested by the way chips almost fly off the ice at the slightest fracture. This is undoutedly caused by the release of compressed air from the bubbles into the fracture.

Either the gas bubbles in a iceberg could be atmospheric air trapped at the time snow was compacted into glacier ice, or, since gases are insoluble in ice (*1*), the bubbles could be frozen out of air-saturated water, as they are in ice cubes from a refrigerator. Water equilibrated with air at 0°C contains 2.9 percent by volume of dissolved gases, of which 34.9 percent is oxygen. Since air has only 20.9 percent oxygen, the concentration of this gas in the bubbles may tell whether the ice was formed by compacting the snow crystals or by freezing of a body of water (*2*).

The rate of gas diffusion through ice is no more than 1/40,000 to 1/70,000 as fast as it is through water (*1*). Considering this extremely slow rate, the relatively enormous diffusion distances in the glacier, and the large quantity of gases held under pressure in the ice, it would seem possible that gas trapped in the glacier would remain unchanged for millenia. Analysis of such gas could therefore give information about the atmospheric composition at the time the ice was formed.

This article (*3*) presents studies on pieces of icebergs taken on board the research vessel *Blue Dolphin* along the Labrador coast. Most icebergs in this area are of Greenland origin. In the interior of Greenland and the Antarctic, the temperature stays below freezing all year, and the glacier ice is formed by the compacting of snow under high pressure. These are the high polar glaciers. In glaciers of warmer climates, melt water percolates through the snow in the summer and freezes deeper down, as an important part of the firnification process (*4*). The gas in such ice should accordingly be more or less enriched with oxygen. Only the polar type of glacier would therefore seem suitable for possible clues to the composition of ancient atmospheric air. Isotope distribution could probably be studied in either type.

Although the techniques for obtaining samples from bubbles in icebergs have been generally adequate, the composition of the gas has been found by several authors to be more or less close to that of the atmosphere, and it has long been known that the gas is usually under pressure (*5*). In our work, we melted a piece of ice in mercury. The gas phase and the dissolved gases in the melt water were analyzed separately and the results were totaled.

A piece of berg ice was shaved to fit snugly into the barrel of a 20-ml syringe. The plunger was set in and mercury drawn in to cover the ice. The first milliliter of melt water and bubbles was discarded. The nozzle was closed with the finger, and the ice-and-mercury volume was read. The ice was quickly melted and a new volume reading taken. The gas phase was transferred to a tuberculin syringe to determine the volume, and it was analyzed for composition (*6*). The volume of meltwater w and mercury was read on the syringe and 1 ml of water was analyzed for dissolved oxygen and nitrogen (*7*). Carbon dioxide could not be determined accurately with the methods we had available. About 85 percent of the total amount of gas analyzed was in the gas phase.

The pressure of the gas in the ice was found as

$$g/x$$

where x is the volume of the compressed gas in the ice and g is the volume at 1 atm. This can be computed according to the formula

$$g/x = \frac{g}{v - 1.091w}$$

where v is the volume of ice and bubbles and $1.091w$ is the volume of ice alone.

It can be estimated that the combined accuracy of the various measurements will amount to about ± 0.2 percent by volume for the total oxygen and nitrogen. The pressure estimates are probably valid to within ± 25 percent.

Thirty pieces taken from six different icebergs were analyzed. It will be seen from Table 1 that the oxygen content in all of the bergs is close to that of the atmosphere, that is, 20.9 percent. Nevertheless, the oxygen content of iceberg No. 5 and especially No. 6 was significantly lower. One may speculate that when the snow settled on the Greenland icecap ages ago and compacted into these pieces of glacier ice (No. 5 and No. 6), an atmosphere was trapped that is slightly lower in oxygen content than our present atmosphere (*8*). Possibly this ice was formed as far back as Pleistocene time, when cold climates may

Table 1. Gases in iceberg ice. Air-equilibrated water at 0°C contains 2.9 percent gas by volume, of which 34.9 percent is oxygen. Clear ice contains less than 0.003 percent gas, most likely none at all (*1*). The pressure determinations are based upon from two to eight analyses in each iceberg.

Iceberg No.	Ratio of compressed gas to ice (ml/100 ml)	Ratio of gas at 1 atm to melt water (ml/100 ml)	Gas pressure in ice (atm)	O_2 in gas (%)
1	1.9 to 2.2	4.2 to 8.3	2.9 to 3.9	21.4, 21.2, 21.2
2	2.3 to 3.8	7.7 to 11.1	2.3 to 3.9	20.9
3	1.2 to 2.2	4.8 to 9.3	2.0 to 6.2	21.2
4	1.1 to 2.6	2.9 to 6.5	1.0 to 5.0	20.6
5	1.0 to 2.4	2.2 to 8.8	3.3 to 5.8	20.2, 20.4
6	2.1 to 5.2	5.6 to 9.9	1.7 to 2.6	20.0, 20.0, 20.1, 20.1